Simulation of Partial Discharge Electromagnetic Wave Propagation in a Switchgear Compartment

Mijodrag Miljanovic[1], Martin Kearns[2], Brian G Stewart[1]

[1]Department of Electronic and Electrical Engineering, University of Strathclyde, Glasgow, Scotland, UK

[2]EDF Energy, East Kilbride, Scotland, UK

***Abstract*- Partial discharge (PD) is one of the main failure contributors in medium voltage (MV) and high voltage (HV) equipment. Left unattended it can lead to service outages of electrical power system. In the case of air insulated MV switchgear equipment there is still need to identify the most effective placement of sensors for PD detection. To assist in optimizing sensor placement, a three-dimensional (3-D) finite element method (FEM) switchgear compartment model with bus bars is developed to study the propagation of electromagnetic waves generated by PD. The distribution of propagated electric field generated within the bus bar compartment from PD at two different locations is studied in the time domain. The simulations provide an improved understanding of the radiated frequency (RF) propagation signals within the internal design, thus understanding better the complex propagation paths to enable future sensor optimization positions.**

Keywords- switchgear; partial discharge (PD), electromagnetic (EM) wave propagation; finite element method (FEM); bus bar

I. INTRODUCTION

The insulation of medium voltage (MV) and high voltage (HV) equipment in electrical power system infrastructure is naturally prone to partial discharge (PD) activity. Unsurprisingly, each component in the infrastructure has a specific noise floor of PD activity during normal operation which is not considered to be harmful. Due to environmental influences and insulation depreciation issues, PD activity levels can rise. Higher PD development reduces the insulation capability of the system and failures can ultimately occur. To avoid such unforeseen occurrences the trend of PD activity can be monitored to reveal the condition state of components. In the case that specific PD levels exceed certain thresholds for the equipment, measures can be taken to avoid failure service outages and permit inspections and repairs to be undertaken.

Generally, there are two different approaches to monitor PD in electrical power equipment. The first approach is the conventional method described by the IEC [1] and IEEE [2], [3] standards. These so-called conventional tests are mainly applied during acceptance tests or prior commissioning. Since these kind of tests are quite extensive, they often require large test equipment, therefore, they are not practical for routine use. For this reason, more practical everyday monitoring methods have been developed which are described as non-conventional methods for example in IEC technical specification 62478 [4]. With respect to switchgear, the application of these non-conventional methods is described in a CIGRE technical brochure [5]. The two main methods applied in MV switchgear are the UHF method using antenna sensors, and HF/VHF methods such as transient earth voltage (TEV) sensors and high frequency current transformers (HFCTs). Both of these methods are based on electric field detection along switchgear compartments or switchgear line-ups. Because of the uncertainty in where to place the sensors most effectively along the compartment, the electric field propagation requires further study to understand better the optimal positions of sensors.

Some previous research has been undertaken on how to effectively distribute sensors along an air insulated medium voltage switchgear, for example in [6]. The propagation of UHF signals and the attenuation characteristics of different components in the frequency domain was investigated in [7]. In [8], the measured UHF amplitude with an excitation pulse was investigated. Investigation of different PD pulse widths on detected HF/VHF amplitude was also performed in [9]. The investigation of radiation pattern based on the EM spectrum was undertaken in [10]. A natural conclusion from all the above research is that there are different power levels at different locations and that these positions are also dependent on the orientation and the structure of the switchgear compartment.

In the work above, the investigations of PD EM propagation was conducted through a single PD source. Often, many PD sources may be present at the same time from different locations. The question then arises of how does the situation change when more than one PD source occurs in the equipment. To understand better the EM propagation from PD sources, this work simulates and investigates the EM fields as a number of sensor probe position for a single PD source at two different locations; it also compares the fields when two PD sources co-exist but taking place at slightly different times. A 3-D simulation model of a practical air insulated MV switchgear bus bar compartment is created for the investigations. The model also has the ability to add PD sources at any location with different PD current injection directions or orientation. The simulation model is described in the following section.

II. SIMULATION MODEL

The 3-D switchgear model is developed in Comsol Software and is shown in Fig. 1. The switchgear is composed of five main compartments, i.e. auxiliary, circuit breaker, bus bar, current transformer and cable compartments. In this particular simulation study, the bus bar compartment is the focus of the investigation. This compartment includes bus bar supports and

conductors as shown in Fig. 2. The supports are modelled as epoxy resin insulation and the 3 phase bus bars are modeled as double bare copper conductors. The enclosure of the busbar compartment is modelled as 3 mm solid aluminum. The PD sources are placed at the so-called "triple junction points", which is the boundary between the conductor, the insulation and air. This point has previously been identified as the most likely position for PD to occur in such equipment [11].

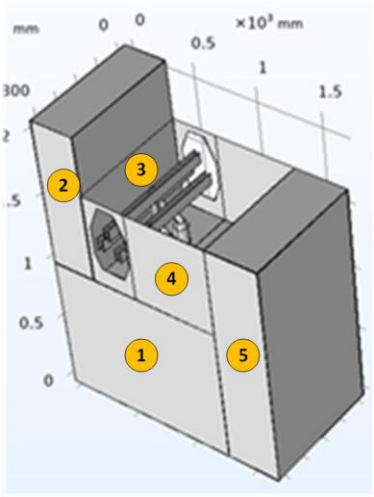

Fig. 1. Switchgear model compartments: (1) Circuit breaker; (2) Auxiliary; (3) Bus bar; (4): Current transformer; (5): Cable.

To simulate the model in the time domain the *EM Wave Transient node* was applied in Comsol. The PD source is implemented by a user defined, rectangular lumped port. A lumped port defines the spot where the PD energy enters the model. A PD current pulse $i_{PD}(t)$ is implemented as a normalized Gaussian pulse [12] as described in (1)

$$i_{PD}(t) = I_0 * e^{-[\frac{(t-t1)^2}{2*\tau^2}]} \qquad (1)$$

where I_o is the peak current, which is set to 1A, and may be applied in all three field component directions as appropriate; the time occurrence of maximum current of the PD source is determined by t_i, and τ represents the pulse width parameter, permitting different PD pulse widths to be produced. In the simulations undertaken, the pulse width was set to 1 ns.

Fig. 2 depicts a top-down view of the bus bar compartment in the 3-D model incorporating three electric field sensor probes. Probes 1 and 2 are placed at the center of the front and the rear sidewalls of the compartment, respectively. Probe 3 is placed at the center of the top of the compartment. The probes detect the field components, [N.1] = E_x, [N.2] = E_y, [N.3] = E_z. The PD sources are applied as shown on phases L1 and L3. The orientation of the PD current injection on each phase is indicated by the small red arrows in Fig. 2.

For the simulations, the *PARDISO* solver with *Generalized alpha* time step was implemented. The simulation step time is 1 ps.

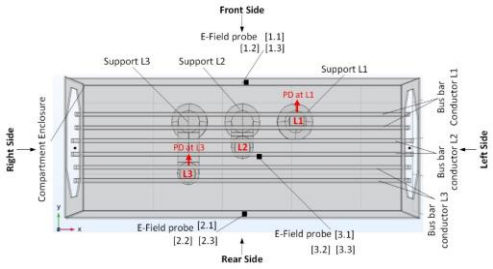

Fig. 2. Busbar compartment (top view), E-field probes and PD sources.

III. Simulation Results

A. *Propagation of EM field in bus bar compartment*

Three different simulations are performed and compared. First, a single PD source applied at the support of phase L1, second, a single PD source applied at the support of phase L3 and third, both PD sources L1 and L3 applied with a time delay of 2.5 ns between each other.

Figs. 3(a) to 3(f) shows the side-left view of the bus bar compartment and the electric field propagation at different time instances. The field displayed in the plots is the E_{norm} field, which is defined as:

$$E_{norm} = \sqrt{E_x^2 + E_y^2 + E_z^2} \qquad (2)$$

Fig. 3(a) depicts the time when PD starts on phase L1. Fig. 3(b) shows the field propagation at 10 ns. The PD on phase L3 starts at 6.5 ns as shown in Fig. 3(c). The propagation of that field can be seen in Fig. 3(d) at a time of 10 ns.

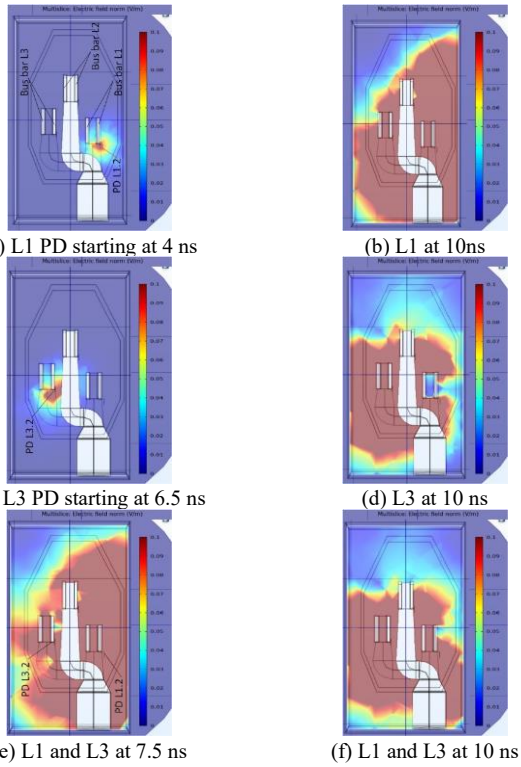

(a) L1 PD starting at 4 ns (b) L1 at 10ns

(c) L3 PD starting at 6.5 ns (d) L3 at 10 ns

(e) L1 and L3 at 7.5 ns (f) L1 and L3 at 10 ns

Fig. 3. E-field distributions from side-left view for L1 and L3 at different times

Figure 3(e) shows the superposition of the two PD sources in the compartment. A residual electric field at 7.5 ns still exists from the PD occurring on phase L1 when the second PD starts on phase L3. Fig. 3(f) shows the distribution of the E field at 10 ns. The plots above show that in all cases, the propagated E field distribution concentrates in the middle of the compartment rather than at the top due to the nature and geometry of the bus bars and metallic enclosure.

B. Probe measurements from PD at phase L1

Figs. 4(a) to 4(c) show the probe E-field components generated by the PD on phase L1. The PD current maximum occurs at 5 ns. The direction of the PD current injection is towards the front side as indicated in Fig. 2. The E_y field component, Fig. 4(b), dominates compared to E_x, and E_z field components as seen in Figs. 4(a) and 4(c), where its amplitude is around two magnitudes higher. It can also be seen that the detected field by probe 1 is generally higher compared to the other two probes due to its close proximity to the PD source.

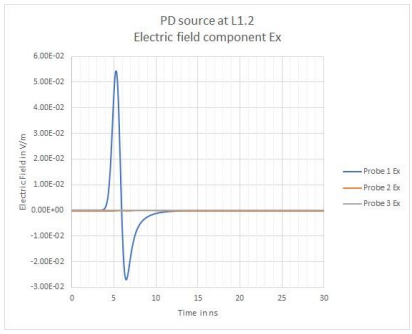

(a) E_x field components from probes 1, 2 and 3

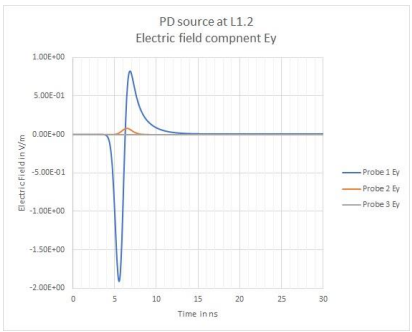

(b) E_y field components from probes 1, 2 and 3

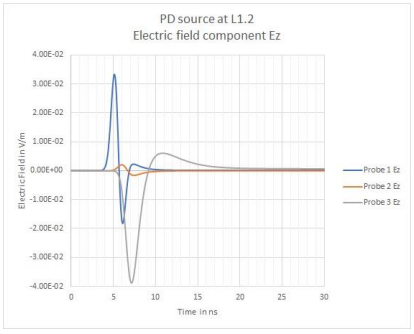

(c) E_z field components from probes 1, 2 and 3

Fig. 4. Probe electric field components for PD on phase L1.

Comparing the probe measurements in Figs. 4(c) with 4(a) and 4(b), the E_z component of probe 3 is the dominant field. This probe is positioned at the very top of the compartment and because of the different field propagation plane, this particular field component becomes distinctive.

C. Probe measurements from PD at phase L3

The PD source was applied on phase L3 with current injection direction towards the front side. The PD pulse current maximum is centered at 7.5 ns. The detected E fields are displayed in Figs. 5(a) to 5(c). It can be seen that E_y is the dominant component. In this case, probe 2 detects the highest field due to its close proximity to the PD source. As seen previously, the E_z field component becomes characteristic for probe 3 due to the alignment of this sensor plane.

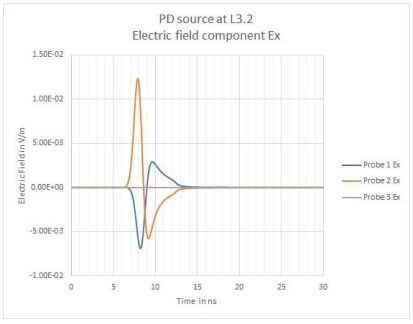

(a) E_x field components from probes 1, 2 and 3

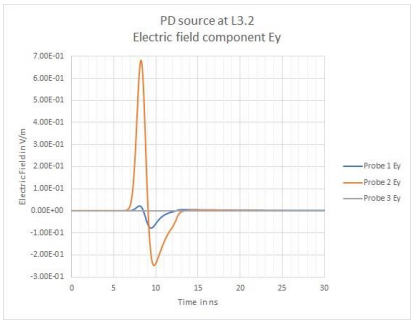

(b) E_y field components from probes 1, 2 and 3

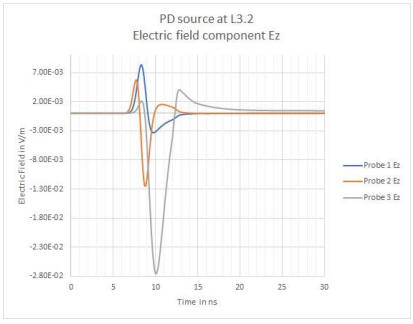

(c) E_z field components from probes 1, 2 and 3

Fig. 5. Probe electric fields for PD on phase L3.

C. Probe measurements from PD sources at L1 and L3

Two PD sources were applied together. The probe electric fields are shown in Figs. 6(a) to 6(c). The occurrence of the two

different PD events and the field superpositions can be clearly distinguished in the graphs. The EM signal superposition in the E_x field component of probe 1, Fig. 6(a), begins close to the start of the PD on L3. There is no superposition in E_x of probe 2 in Fig. 6(a) since no significant E_x field is detected for PD on L1, Fig. 4(a). E_x of probe 2 occurs identically to the case of the single PD on L3 situation, Fig. 5(a).

Field superposition exists in the E_y and E_z field components. The E_y field component is again dominant at the sidewalls of the compartment as seen Fig. 6(b), compared to E_x and E_z components. It is again about two magnitudes higher. It seems also that the highest field is detected by probe 1 compared to probes 2 and 3. This is most likely due to the orientation of the PD sources to the front wall where probe 1 is placed.

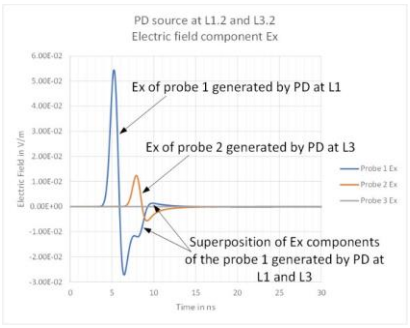

(a) E_x field components from probes 1, 2 and 3

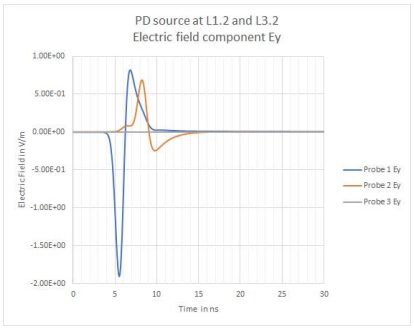

(b) E_y field components from probes 1, 2 and 3

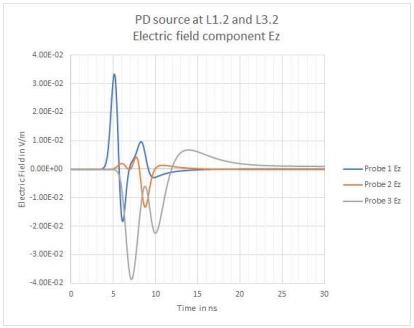

(c) E_z field components from probes 1, 2 and 3

Fig. 6. E field detection for two PD sources on phases L1 and L3

IV. Conclusions

Through simulation, it has been shown that the propagated EM field distribution generated from PD sources with different current injection orientations and directions can be studied. For the cases of the two PD sources investigated, with current sources orientated in the same direction, the radiated fields are concentrated towards the middle sections of the compartment.

For these PD sources, the E_y field is the dominant component at the sidewalls of the cabinet, whereas due to the different sensor plane, the E_z component dominates on the very top surface of the compartment. As expected, the PD EM propagation nature varies depending on PD location position and the nature of insulation and metallic structure boundaries.

For the case of two PD sources co-existing in the compartment, superposition of the field components exists, thus changing the nature of the detected fields. The superposition of different PD EM can ultimately be complex in nature. To this end, simulation studies will enable an evaluation of the complexity of EM propagation in bus bar compartments, permitting an understanding of how best to discriminate potential single and multiple PD sources arising from critical insulation degradation positions in the compartment.

Future work will involve evaluating EM propagation modes for PD sources with current injections in different directions, as well as understanding the impact on probe measurement fields for PD pulses with different pulse widths. The ultimate aim of the project is the development of an online condition monitoring system for MV bus bars.

References

[1] IEC EN 60270, *High-voltage test techniques -Partial discharge measurements*, IEC, April 2016.

[2] IEEE *Guide for Partial Discharge Measurement in Power Switchgear*, IEEE Std. 1291-1993, March 1993.

[3] IEEE *Recommended Practice for Partial Discharge Measurement in Liquid-Filled Power Transformers and Shunt Reactors*, IEEE Std. C57.113-2010, August 2010.

[4] IEC/TS 62478:2016, *HV test techniques - Measurement of partial discharges by electromagnetic and acoustic methods*, IEC, August 2016.

[5] Joint Work Group A3.32/CIRED, *Non-Intrusive Methods for Condition Assessment of Distribution and Transmission Switchgear*, CIGRE/CIRED, August 2018.

[6] Marco Tozzi, *Partial Discharge in Power Distribution Electrical Systems: Pulse Propagation Models and Detection Optimization*, PhD Thesis, University of Bologna, 2010.

[7] C. Yao, C. Huang, Y. Chen, P. Qiao, *Study on the Application of an Ultra-High-Frequency Fractal Antenna to Partial Discharge Detection in Switchgears*, Sensors, December 2013.

[8] H. Luo, H. Liu, K. Kang, P. Cheng, F. Yang, Q. Yang, *Investigation of Propagation Characteristics of UHF Electro-magnetic Wave Due to PD in Switchgear*, IEEE 11th Conference on Industrial Electronics and Applications (ICIEA), Hefei, China, October, 2016.

[9] Y. Li, Y. Wang, G. Lu, J. Wang, J. Xiong, *Simulation of Transient Earth Voltages Aroused by Partial Discharge in Switchgear*, International Conference on High Voltage Engineering and Application, New Orleans, USA, November, 2010.

[10] B. Zheng, A. Bojovschi, X. Chen, *Electromagnetic Radiation Spectrum from Partial Discharge in Air-Insulated Medium Voltage Switchgear*, Power Engineering and Automation Conference, Wuhan, China, September, 2012.

[11] M. El-A. Slama, A. Beroual, A. Girodet and P. Vinson, *Creeping Discharge and Flashover of Solid Dielectric in Air at Atmospheric Pressure: Experiment and Modelling*, IEEE Transactions on Dielectrics and Electrical Insulation, October 2016.

[12] T. Zhao, M.D. Judd, B.G. Stewart, *Time Dependent Simulation of PD Electromagnetic Wave Propagation*, Annual Conference on Electrical Insulation and Dielectric Phenomena (2020): CEIDP 2020.